Proceedings of

The Twenty-Sixth Symposium
on Naval Hydrodynamics

Rome, Italy
September 17–22, 2006

The Resistance Components of a Surface-Effect Ship

Lawrence J. Doctors

School of Mechanical and Manufacturing Engineering
The University of New South Wales
Sydney, NSW 2052, Australia

Chris B. McKesson

JJMA Naval Architecture Division
Alion Science and Technology
Silverdale, WA 98383, USA

Compiled on May 16, 2006

ONR '06

Twenty-Sixth Symposium on Naval Hydrodynamics
Rome, Italy, September 17–22, 2006

The Resistance Components of a Surface-Effect Ship

Lawrence J. Doctors (The University of New South Wales, Australia)
Chris B. McKesson (Alion Science and Technology, USA)

Abstract

The research described here includes enhancements to the theoretical analysis of the resistance components of a surface-effect ship (SES). The resistance predictions are verified against extensive tests on an SES model in a towing tank.

Specifically, the new analysis includes two prediction methods. The first method is aimed at the stern seal, which is normally constructed as a multilobed inflated structure. The second method is applicable to the bow seal, whose lower part (at least) is composed of a row of flexible fingers which are assumed to deflect backward in order to accommodate changes in water level relative to the craft. The deflected part of the fingers is modeled as a planing surface. These theories are applicable to the case when the SES is operated in the partial-cushion mode and the seals are deliberately dragged through the water.

It is shown that the frictional resistance on either the stern seal or the bow seal is a relatively unimportant component of the total resistance budget.

However, the pressure resistance on the bow seal is certainly significant. For example, at a Froude number of 0.2, when the model was deliberately operated in a partial-cushion mode with the seals in substantial contact with the water, the effect of the presence of the seals is to more than double the overall resistance of the vessel. At a Froude number of 0.35, the seals still increase the total resistance by at least 15%.

It is clearly worthwhile to avoid such resistance penalties; this aim can be achieved by use of the new prediction techniques explained here.

1 Introduction

1.1 Background

It is clear that, in order to achieve substantial increases in over-water speed, it is necessary both to minimize the wave resistance and to essentially eliminate the frictional resistance. The surface-effect ship (SES) represents a serious attempt to achieve this dual aim. This concept was described by Ford (1964) and Ford, Bush, Wares, and Chorney (1978), and many others.

In addition to the desire to achieve high speeds of operation, it is a frequent requirement that the vessel operate efficiently at low speed, such as in formation with a fleet. That is, the operator is prepared, during certain phases of the use of the vessel, to sacrifice speed hopefully without excessive fuel consumption.

The reduction of speed is always a very effective method for lowering the fuel consumption in the case of traditional displacement vessels. However, this may not be the case for an SES. The cause of this deficiency is the uniform cushion pressure (supporting most of the weight of the vessel), which can generate a substantial wave system at low speeds resulting in a large wave resistance. This particular problem can be addressed, at least in part, by considering a split cushion in which differential pressures are utilized. This approach has been detailed in previous research by Doctors (1997), Doctors and Day (2000), and more recently by Doctors, Tregde, Jiang, and McKesson (2005).

The latter paper is particularly interesting because it was demonstrated that traditional linearized wavemaking theory — essentially based on the landmark paper by Michell (1898) — could pro-

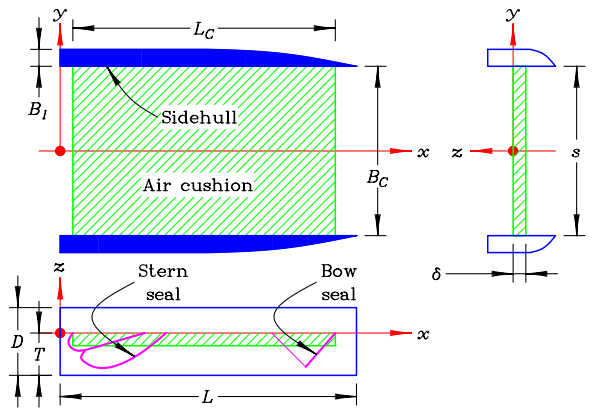

Figure 1: Definition of the Problem
(a) Single-Cushion SES

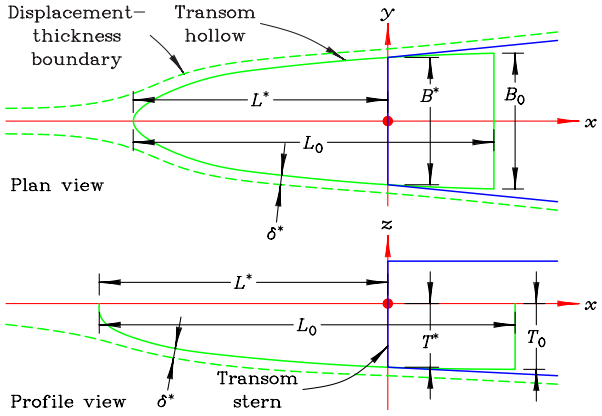

Figure 1: Definition of the Problem
(b) Estimation of Hollow Length

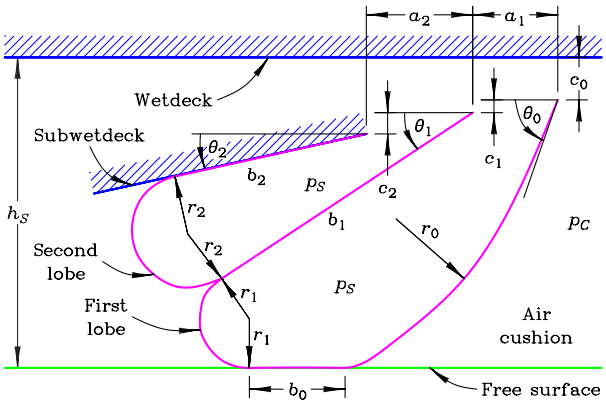

Figure 1: Definition of the Problem
(c) Stern Seal

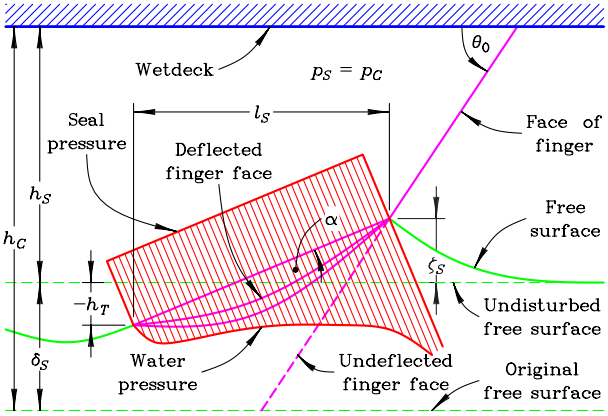

Figure 1: Definition of the Problem
(d) Bow Seal

vide excellent prediction of the resistance characteristics of the vessel. The exception to this statement is that the theory substantially underpredicted the resistance of the model SES in the low-speed hump region.

It was recognized by Doctors, Tregde, Jiang, and McKesson (2005), that the cause of this underprediction was the fact that the resistance of the seals was ignored in the analysis. This could be a significant factor when the model was operated in a partial-cushion mode with the seals dragging in the water. It was this recognition that provided the incentive behind this current study.

All of these matters affect the overall hydrodynamic efficiency of the vessel, which is usually defined through the effective lift-to-drag ratio or, alternatively, the transport efficiency. The quest to improve transport efficiency is, in fact, the driving force behind this project. This concept was first introduced to the engineering community by Gabrielli and von Kármán (1950), who demonstrated that different transport vehicles offered varying efficiencies which generally became lower for the higher speeds being contemplated. The transport factor was explained in detail by Kennell (2001). Comparisons between different types of vessel, specific to the marine environment, have been made by Templeman and Kennell (1999) and Broadbent and Kennell (2001).

A reader interested in some of the early work done on model SES vessels may wish to consult the publications by Heber (1974), Di Joseph, Heber, King, and Wilson (1975), and Wilson, Wells, and

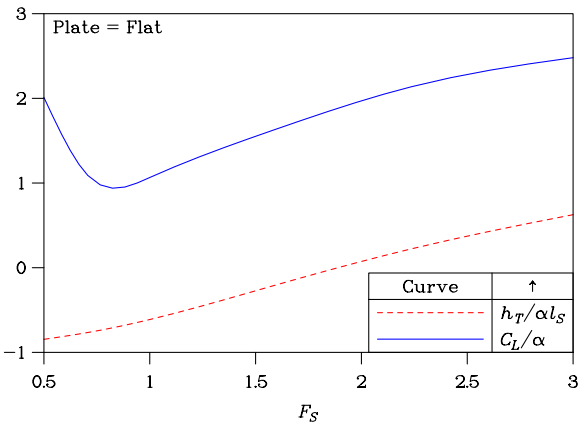

Figure 2: Rise Height and Lift Coefficient of Planing Bow Seal

Heber (1979). Work specific to the fingers on an SES bow seal was described by Malakhoff and Davis (1981). Layton (1976) performed tests on a model bow seal that consisted of a double lobe fitted with a semirigid lower planing surface, with the purpose of seeking the optimal shape of the semirigid element in order to minimize the resistance of the vessel. Van Dyck and Fridsma (1979) were responsible for a very extensive set of tests on a model SES which was equipped with stern and bow seals built into independent modules — thus permitting measurements of the resistance on the two seals separately from the resistance on the entire vessel.

1.2 Current Work

It was decided here to construct a theory that would model the behavior of the two seals of the SES, within the framework of simple physics and linearized free-surface theory. In the present context, it was considered to be necessary to avoid the complications of computational fluid dynamics (CFD), which would change the whole philosophy of developing and enhancing a computer code that can accurately predict the performance of a high-speed vessel within a second of central-processor unit (CPU) time on a computer.

This is not to say that a CFD program could not be used in a very effective manner to study the details of the complex flow in the vicinity of SES seals.

The basic features of the SES are depicted in Figure 1(a). The intention here is to model the hydrodynamics of the sidehulls, the cushion, the stern seal, and the bow seal. The nature of the water flow past the transom demisterns is indicated in Figure 1(b).

Of course, it is necessary to be assured that the linearized hydrodynamics are an adequate representation of the real water flow. To this end, Doctors, Renilson, Parker, and Hornsby (1991) demonstrated that such resistance predictions are sufficiently accurate for engineering purposes, such as design and optimization. This effort was continued by Couser, Molland, Armstrong, and Utama (1997). Yet another such comparison between linearized predictions of resistance and experimental measurements was conducted by Sahoo and Doctors (2003) for a high-speed monohull in water of restricted width and depth.

The linearized free-surface theory will be applied to both the (solid) part of the SES (as noted above), the air cushion, and the planing behavior of the deflected bow seal. This planing theory was first developed by Sretensky (1933), Maruo (1951), and Squire (1957), amongst many others.

2 Theory of the Behavior of a Seal

2.1 Stern Seal

Figure 1(c) presents the essential features of a typical stern seal fitted to an SES. For simplicity, the diagram shows a two-lobe seal. However, it is more usual for an SES to be fitted with a three-lobe seal, as was the case for the subject model in the current work.

It is assumed that the cushion pressure p_C is uniform and that the seal pressure p_S is also uniform and is the same within each lobe in the seal. This latter assumption restricts the present analysis to steady-state conditions only. A dynamic model (that is, a seakeeping model) would need to account for the pressure differentials that can be set up between the individual lobes within the stern seal. It is not clear, without developing this more sophisticated unsteady model of the stern seal, just how important such dynamic effects would be.

In practice, the seal is pressurized by a fan system separate from that used to supply the air cushion. The details of these fans have been omit-

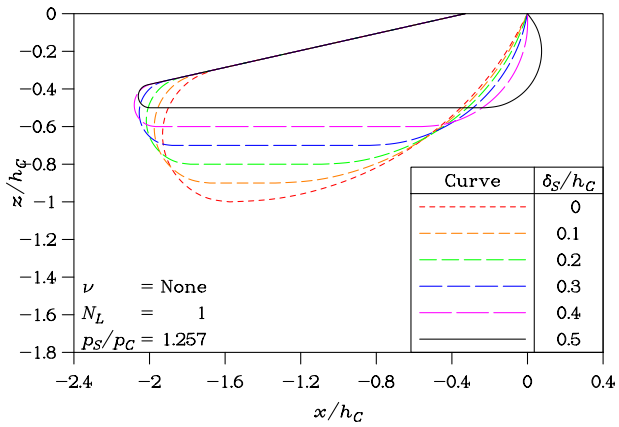

Figure 3: Deflection Behavior of Stern Seal (a) One-Lobe Seal (Inviscid)

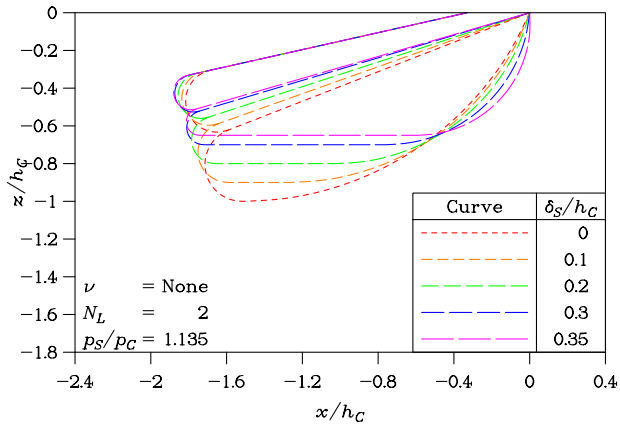

Figure 3: Deflection Behavior of Stern Seal (b) Two-Lobe Seal (Inviscid)

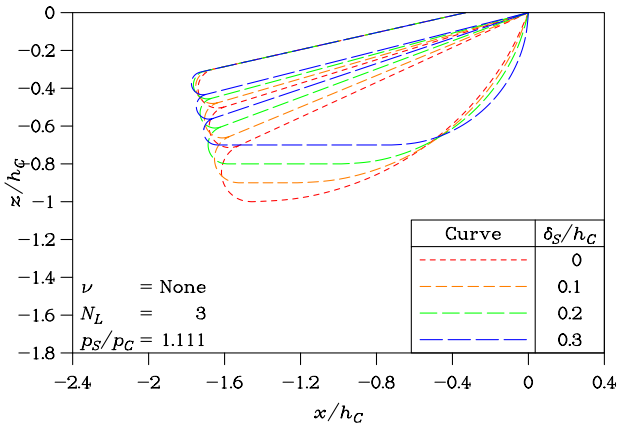

Figure 3: Deflection Behavior of Stern Seal (c) Three-Lobe Seal (Inviscid)

ted from this figure. The height of the seal after deflection by the water is h_S.

The parameters defining the first (front) lobe are: the length of "flat" b_0 where the lobe contacts the water, the radius of curvature of the lobe face r_0, the angle of the lobe face θ_0, the length of flat b_1 where the lobe contacts the second lobe, the radius of curvature of the lobe back r_1, and the back angle θ_1. Additional dimensional information defining the attachment points for the lobe ends includes c_0, a_1, and c_1 for the first lobe, and b_2, r_2, θ_2, a_2 and c_2 for the second lobe. Finally, to complete the definition of the geometry, one must state the lobe perimeters l_1 and l_2.

A third lobe (not shown here), would be defined by the additional corresponding six parameters, b_3, r_3, θ_3, a_3, c_3, and l_3.

The first equation describing the equilibrium of the first lobe refers to the longitudinal forces which must sum to zero. That is, $f_1 = 0$:

$$f_1 = (p_S - p_C)r_0 - p_S r_1 - f_S \frac{1}{2}\rho U^2 b_0 (C_F + C_A)\,. \quad (1)$$

Here, ρ is the density of the water, U is the speed of the vessel, C_F is the friction coefficient for the seal surface, and C_A is a correlation allowance. Also, an overall seal roughness factor f_S has been included to allow for additional resistance effects, such as spray, not included in this analysis.

There are also four equations of geometry for the first lobe. Assuming that the equations are satisfied, the functions $f_2, \ldots, f_5$ are each zero:

$$f_2 = -b_1 \cos\theta_1 + r_1 \sin\theta_1 + r_0 \sin\theta_0 + b_0 - a_1\,, \quad (2)$$

$$f_3 = b_1 \sin\theta_1 + r_1(1 + \cos\theta_1) + c_0 + c_1 - h_S\,, \quad (3)$$

$$f_4 = r_0(1 - \cos\theta_0) + c_0 - h_S\,, \quad (4)$$

$$f_5 = b_0 + b_1 + r_0\theta_0 + r_1(\pi - \theta_1) - l_1\,. \quad (5)$$

There are three equations of geometry for the second lobe. Assuming that these equations are satisfied, the functions f_6, f_7, and f_8 are each zero:

$$f_6 = b_1 \cos\theta_1 - b_2 \cos\theta_2 + r_2(\sin\theta_1 + \sin\theta_2) - a_2\,, \quad (6)$$

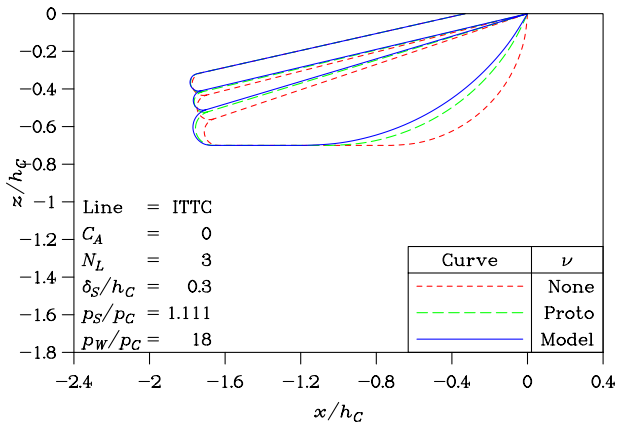

Figure 4: Influence of Water Friction on Stern Seal

$$f_7 = b_1 \sin\theta_1 - b_2 \sin\theta_2 - r_2(\cos\theta_1 + \cos\theta_2) - c_2 \,, \quad (7)$$

$$f_8 = b_1 + b_2 + r_2(\pi + \theta_1 - \theta_2) - l_2 \,. \quad (8)$$

For each additional lobe, there will be an additional corresponding three unknowns and an additional corresponding three equations. If one considers the angle of the subwetdeck to be known, the number of equations equals the number of unknowns and the resulting set of equations can be solved, in principle.

The Newton-Raphson method was employed for this purpose. It is a simple matter to derive the analytic expressions for the relevant gradients of the above functions f, where we seek to find their zeroes. It is also necessary to find a suitable starting point for the iterations. Finally, it was found crucial to apply a *relaxation factor*, less than unity, to the computed changes in the values of the variables in order to ensure stability of the Newton-Raphson iteration. It was also found possible to improve (increase) the resulting slower convergence rate by allowing this relaxation factor to return to unity as the solution was approached.

2.2 Bow Seal

Figure 1(d) illustrates the main features of a finger bow seal. We assume that the fingers deflect backwards at the water surface in a simplistic manner as shown. The shape of the lower part of the fingers is critical to the analysis. For the present,

Table 1: Resistance Components

Symbol	Meaning
R_A	Correlation resistance
R_F	Frictional resistance
R_H	Hydrostatic resistance
R_L	Lift resistance
R_M	Momentum resistance
R_S	Seal resistance
R_T	Total resistance
R_W	Wave resistance
R_{air}	Air resistance

we shall consider that the fingers possess a sufficient level of stiffness so that they create a planing surface, which is flat in the first instance. Alternatively, we might consider that the fingers adopt a parabolic or cubic profile.

The seal pressure p_S acting on the rear surface of the fingers equals the cushion pressure p_C. The finger angle relative to the wetdeck is θ_0 and the vertical deflection of the lower edges of the fingers is δ_S. The planing length of the fingers is l_S and the trailing edges of the fingers are at a height (usually negative) h_T above the undisturbed free surface. The unknown planing angle is α.

The analysis can proceed by utilizing standard planing theory. This theory has been developed over a number of years in the last century. Typical landmark papers in the field are those written by Sretensky, Maruo, and Squire. A very easy approach to the two-dimensional planing problem was suggested by Doctors (1974), who used overlapping triangular "tent" pressure elements acting on the surface of the water in order to model the action of the planing surface.

Typical results for the case of an assumed flat planing surface in this paper are reproduced in Figure 2. The solution to the problem makes use of influence functions (the wave elevation generated by a pressure element of unit value), so that one obtains a linear set of equations for the unknown pressures as well as the unknown planing elevation h_T of the trailing edge. This approach is based on assuming that the planing length l_S is known beforehand, which is generally not the case. Consequently, one must then iterate the otherwise linear theory to obtain the planing length required to support the specified load.

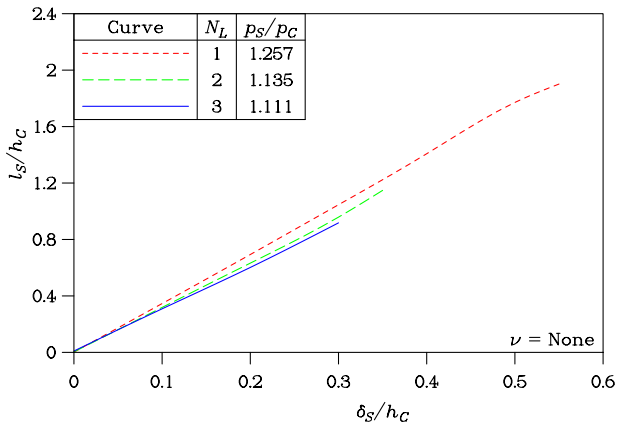

Figure 5: Characteristics of Stern Seal (Inviscid) (a) Wetted Length

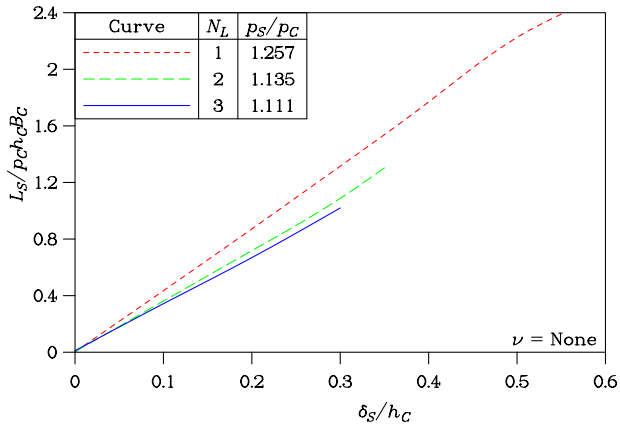

Figure 5: Characteristics of Stern Seal (Inviscid) (b) Direct Lift

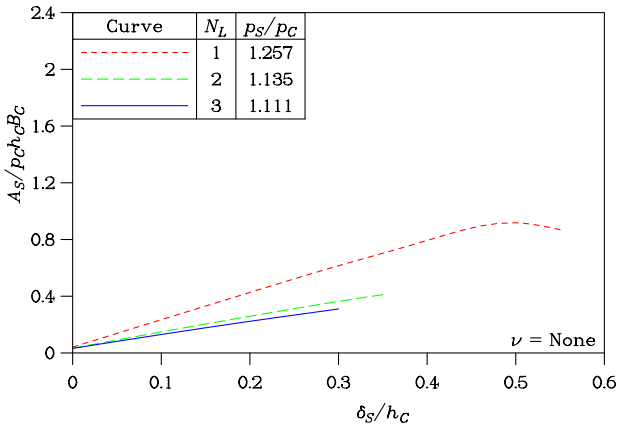

Figure 5: Characteristics of Stern Seal (Inviscid) (c) Total Lift

Figure 2 shows, firstly, the dimensionless rise height of the trailing edge as a function of the seal-wetted-length Froude number $F_S = U/\sqrt{gl_S}$. At low speeds, the ordinate of the curve approaches the value -1, the purely hydrostatic situation. The second curve is the lift coefficient per unit angle $C'_L = C_L/\alpha$. The parameter is often called the *slope of the lift curve*. The curve of C'_L approaches the value π at a high Froude number, which is one half the value obtained from the corresponding theory for the lift of a flat wing (which generates equal lift on its upper and lower surfaces).

The profile of a flat surface is simply:

$$z = \alpha x \,, \tag{9}$$

while a parabolic profile is defined by the equation:

$$z = \alpha x^2/l_S \,, \tag{10}$$

and a cubic profile by the equation:

$$z = \alpha x^3/l_S^2 \,. \tag{11}$$

It can be seen from Figure 1(d) that the wetted seal length is:

$$l_S = (\delta_S + \zeta_S)/\sin\theta_0 \,, \tag{12}$$

where ζ_S is the rise of the water at the point of deflection.

Next, one can compute the seal-wetted-length Froude number and then use the data in Figure 2 to compute the slope of the lift curve C'_L. After this, one can compute the direct seal lift and the planing angle via the formulas:

$$L_S = p_S(l_S B_C) \,, \tag{13}$$

$$\alpha = L_S/\frac{1}{2}\rho U^2(l_S B_C)C'_L \,, \tag{14}$$

in which B_C is the beam of the air cushion. Finally, the pressure resistance on the bow seal is simply:

$$R_{SP} = \frac{1}{2}\rho U^2(l_S B_C)C_D \,, \tag{15}$$

in which C_D is the drag coefficient. For a flat plate, we have the simple result:

$$C_D = \alpha C_L \,. \tag{16}$$

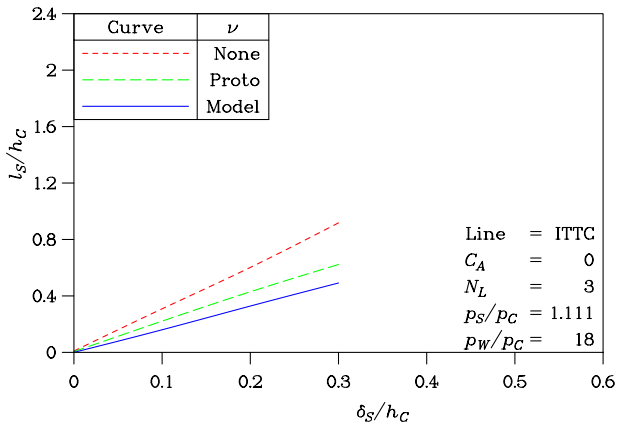

Figure 6: Characteristics of Stern Seal (Water Friction) (a) Wetted Length

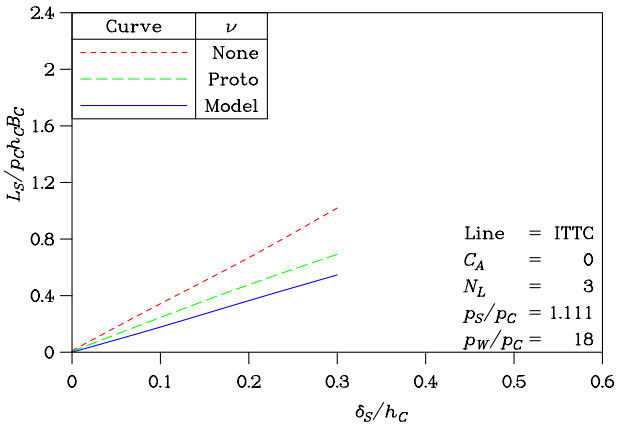

Figure 6: Characteristics of Stern Seal (Water Friction) (b) Direct Lift

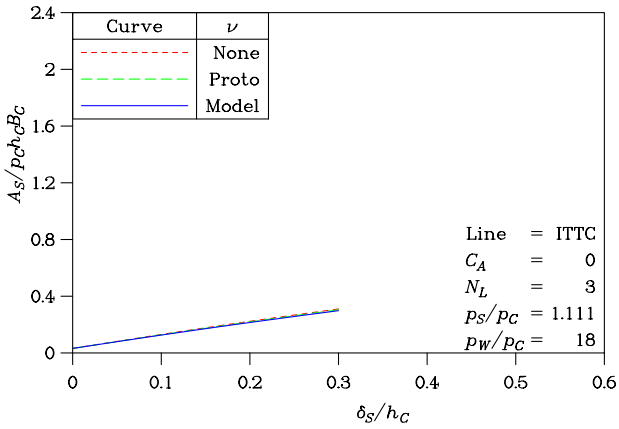

Figure 6: Characteristics of Stern Seal (Water Friction) (c) Total Lift

Because the linear theory of planing becomes invalid as the speed approaches zero, a limiting seal pressure resistance based on hydrostatic considerations is assumed:

$$R_{SP,\max} = \frac{1}{2}\rho g \delta_S^2 B_C \,. \qquad (17)$$

Lastly, one should add the seal frictional resistance R_{SF}, estimated from a suitable formula, such as one of those published by Lewis (1988). That is, the total seal resistance becomes:

$$R_S = R_{SP} + R_{SF} \,. \qquad (18)$$

In order to consider the rise in the water level ahead of the seal ζ_S, its unknown numerical value is first set to zero and the finger is considered to buckle where it would intersect the assumed level of the free surface. From this geometry, one can compute the wetted length of the seal and the lift coefficient per unit angle from the second curve in Figure 2. The planing theory used here works on the basis of an assumed wetted length. As a consequence, the theory provides the rise of the planing surface possessing this planing length. Thus, the first curve in Figure 2 can next be utilized to compute the elevation of the trailing edge of the seal.

In general, this computed trailing-edge elevation from the hydrodynamics of the planing will not equal the elevation derived from the geometry. This implies that one must execute an iteration procedure (in terms of ζ_S) to ensure that the elevation of the trailing edge h_T in Figure 2 matches that from the geometry of the seal. The secant method described by de Vahl Davis (1986) is used here.

2.3 Total Resistance of Vessel

In this research, we shall assume that the resistance of the seals R_S can be added to the other components of resistance in the traditional manner, to give the total resistance R_T, as follows:

$$R_T = f_W R_W + R_H + f_F R_F + R_A + R_S + R_{\text{air}} + R_M \,. \qquad (19)$$

The additional symbols in this equation are the wave-resistance form factor f_W, assumed to be unity in the current work, the wave resistance R_W, the transom-stern resistance R_H, the frictional form factor f_F, and the correlation resistance R_A. The

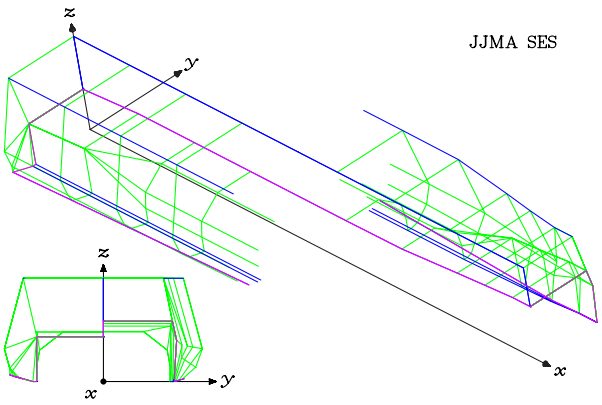

Figure 7: Subject Vessel
(a) Input Mesh

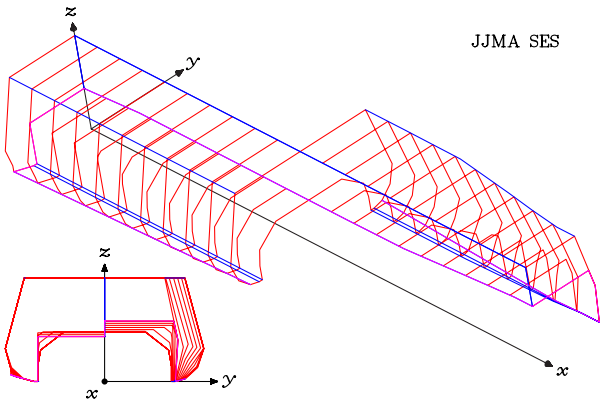

Figure 7: Subject Vessel
(b) Equally Spaced Sections

latter is considered to be zero for a comparison of data from model tests with theoretical predictions run at the same model scale. Also included are the air resistance R_{air} and the momentum resistance R_M. All these resistance components are listed in Table 1.

The reader is referred to Newman and Poole (1962), Doctors and Sharma (1972), and Doctors (1993 and 2003), for the specific formulas for the theoretical wave resistance R_W, which correctly accounts for the interactions between the wave systems generated by the air cushion and by the two sidehulls, within the framework of linearized free-surface theory. There is one proviso, however. The sidehulls are modeled through the use of a source distribution (only), without a transversely directed dipole distribution. Thus, the influence of lateral velocities induced on either sidehull by its twin or by the air cushion is ignored.

3 Results for Stern Seal

3.1 Deflection in Inviscid Flow

We turn our attention to Figure 3 which illustrates the geometry of the stern seal for three different numbers of lobes. Thus, Figure 3(a) shows the effect of the local seal depression δ_S on the shape of a one-lobe seal. All the data has been rendered dimensionless using the cushion height h_C and the cushion pressure p_C. Also indicated on the figure is the seal-pressure ratio p_S/p_C. In this example, we have chosen to ignore the frictional resistance of the water. That is, the last term of Equation (1) has been ignored. One can observe the progressively increasing length of the seal surface which is in contact with the water, as the seal depression is increased.

Figure 3(b) and Figure 3(c) display similar profiles for the case of two lobes and for the case of three lobes, respectively.

In Figure 4, we see a similar plot for the three-lobe stern seal, for different model scales, and for one depression, namely $\delta_S/h_C = 0.3$, only. The first curve, labeled "None", is the inviscid case extracted from Figure 3(c). The second curve, labeled "Proto", refers to the full-size prototype vessel, which is the subject of this investigation. The third curve, labeled "Model", refers to the 1/17.5-scale model. The data pertains to a particular speed (near the maximum speed of 60 knots full-scale), for which the water-pressure-cushion-pressure ratio is: $p_W/p_C = \frac{1}{2}\rho U^2/p_C = 18$.

One can observe that the presence of viscosity is to drag back the seal — not an unexpected result. There is, nevertheless, little difference between the resulting geometry of the prototype seal and that of the model seal.

3.2 Wetted Length and Lift

A primary reason for our interest in the behavior of the stern seal is that the length of seal in contact with the water gives rise to additional and unwanted frictional resistance. This and other matters are considered in Figure 5.

Table 2: Data for Sidehull of SES Concept

Item	Symbol	Value
Displacement mass	Δ	199.32 t
Waterline length	L	80.14 m
Waterline beam	B	3.546 m
Draft	T	1.374 m
Waterplane-area coef.	C_{WP}	0.6903
Maximum section coef.	C_M	0.7244
Block coefficient	C_B	0.4975
Prismatic coefficient	C_P	0.6868
Slenderness coefficient	$L/\nabla^{1/3}$	13.84
Hull-lift ratio	r_{hull}	20 %

Table 3: Data for Cushion of SES Concept

Item	Symbol	Value
Cushion length	L_C	72.000 m
Cushion beam	B_C	17.500 m
Cushion start station	x_1	2.000 m
Long. smoothing factor	α_x	0.150 m^{-1}
Trans. smoothing factor	α_y	0.150 m^{-1}
Number of subcushions	N_C	1
Cushion-lift ratio	r_{cush}	80 %

The wetted length is plotted in Figure 5(a), for the three different numbers of lobes, already referred to. It is extraordinary that the wetted length is very nearly linear with respect to the seal depression — despite the extremely nonlinear nature of the governing equations. It is also remarkable that the number of lobes N_L is almost an irrelevant parameter in this part of our study.

The direct lift force required to depress the seal L_S is plotted in Figure 5(b). Again, the curves are very nearly linear. This point could be considered as quite heartening, because it paves the way to developing a reliable linear theory for the motions of an SES in waves.

Finally, in Figure 5(c), we see the "total lift" A_S. This is the total change in force as a result of the depression of the seal. This force is equal to the direct seal force L_S together with the force on the SES resulting from a change in cushion area (due to the bottom of the seal moving rearward). Again, remarkably, the results are very linear with respect to the seal depression δ_S.

A further implication of these theoretical seal characteristics is that one should be able to ignore the influence of stern-seal friction when developing software for predicting SES motions.

3.3 Influence of Vessel Scale

The three parts of Figure 6 show the same three parameters of interest, namely seal wetted length l_S, direct lift L_S, and total lift A_S. In this case, however, the number of lobes has been set to three, and the influence of water friction (scale of vessel) is studied. The wetted seal length is seen to be less at model scale in Figure 6(a) and, as a consequence, so is the direct seal lift in Figure 6(b). Curiously, the total lift is essentially independent of the scale of the vessel, as seen in Figure 6(c).

4 Exercising the Computer Program

4.1 Subject Vessel

The subject vessel is shown in the two parts of Figure 7. Figure 7(a) is the input mesh employed to describe the hull shape, while Figure 7(b) presents standard views based on 20 equally-spaced sections.

Some of the engineering data specifying the sidehull geometry is also listed in Table 2. This data pertains to the condition of the vessel loaded to a displacement of 1993 tonnes with 80% of its weight borne by the air cushion. Table 3 lists relevant data for the air cushion itself.

4.2 Resistance Components of Vessel

Figure 8 shows the resistance components for the model of the SES. The data for figures is for two different loadings of the vessel, namely "Full" in Figure 8(a) and Figure 8(b) and "Light" in Figure 8(c) and Figure 8(d). The hydrodynamic and aerodynamic components of resistance are separated for this purpose. The *specific* resistance components are plotted. That is, the resistance components are rendered dimensionless using the vessel weight W. Reference may be made to the paper by Doctors, Tregde, Jiang, and McKesson (2005) for a complete explanation of these curves, particularly those plotted in Figure 8(c) and Figure 8(d), the Light-Load

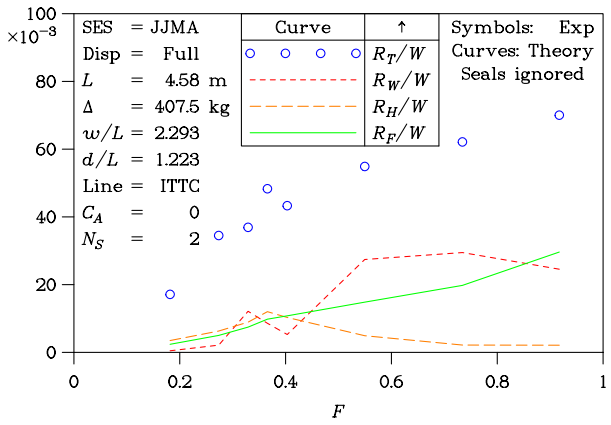

Figure 8: Resistance of Surface-Effect Ship (a) Hydrodynamic Components (Full)

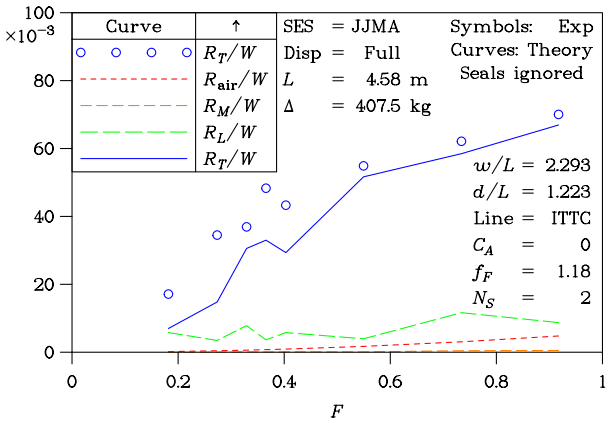

Figure 8: Resistance of Surface-Effect Ship (b) Aerodynamic Components (Full)

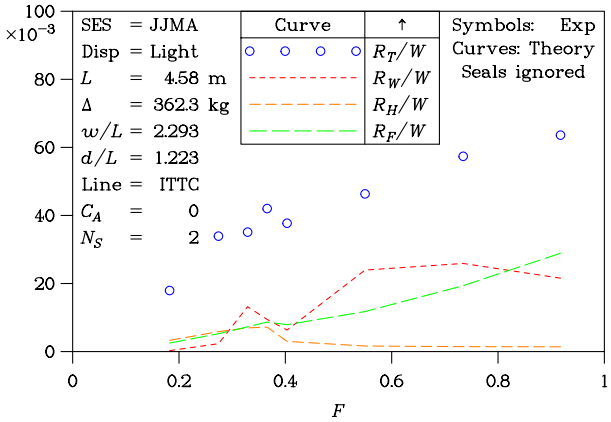

Figure 8: Resistance of Surface-Effect Ship (c) Hydrodynamic Components (Light)

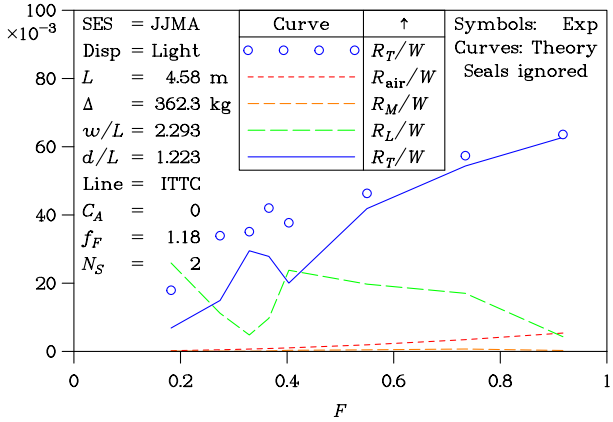

Figure 8: Resistance of Surface-Effect Ship (d) Aerodynamic Components (Light)

condition, which is extracted from that earlier paper. Figure 8(a) and Figure 8(b) are new.

The experimental data for the towing-tank tests was analyzed by Steen (2004).

The main point to observe is the very good agreement between the prediction of the total lift and the experimental data — except in the hump region. It is this discrepancy which forms the heart of the present study.

4.3 Resistance of Seal System

The predictions for the resistance of the seal system are presented in the two parts of Figure 9, for the two loading conditions, respectively.

We consider first Figure 9(a), for the Full-Load condition. The specific seal resistance R_S/W is plotted against the vessel Froude number F. The results from five theories are shown. The first curve, denoted by "Fric", is the resistance suffered by the vessel due to the friction on the stern seal alone (that is $N_S = 1$). The second curve, also denoted by "Fric" (but with $N_S = 2$) shows the frictional resistance suffered by both the stern seal and the bow seal. The third curve, indicated by "F&Flat" is the seal resistance, assuming there is friction on both seals, together with the planing (pressure) resistance of a flat bow seal, according to the theory described in this paper. The fourth curve, indicated by "F&Parab", assumes a parabolic profile of the deflected part of the bow seal. Finally, the fifth curve, indicated by "F&Cubic", assumes a cubic profile.

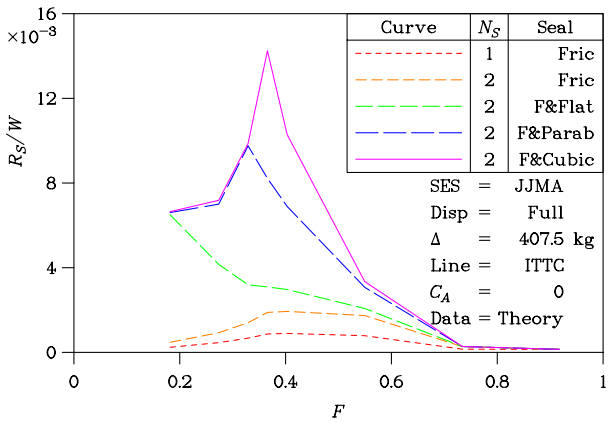

Figure 9: Theoretical Resistance of Seal System (a) Full Displacement

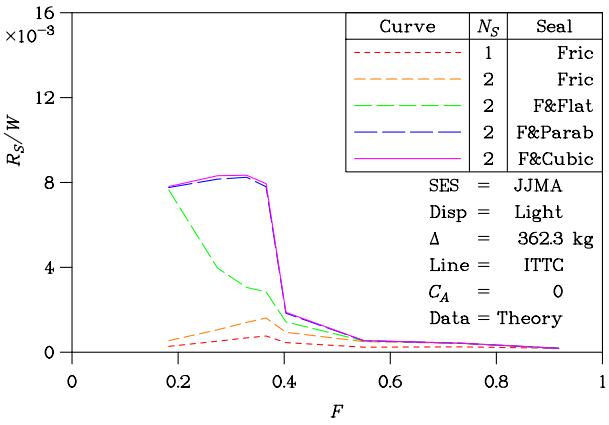

Figure 9: Theoretical Resistance of Seal System (b) Light Displacement

These theoretical predictions indicate that the frictional resistance of the seals is not the major factor — at least at near-hump speeds. Indeed, it is the pressure resistance on the seals that is significant. It is also illuminating to observe that it is important to consider the proper profile of the seals.

The explanation for the increasingly greater resistance of the seals at low speeds is straightforward. Firstly, the water dynamic pressure obviously drops rapidly as the speed is reduced. As a result, the bow seal must adopt an increasingly greater planing angle in order to support the cushion load acting upon it. This effect alone increases the resistance, inversely with the square of the speed, according to Equation (14). Secondly, at these low seal-length Froude numbers (typically about unity), the lift coefficient drops off even further, as seen in Figure 2. This magnifies the phenomenon of the increasing planing angle of the seal.

Similar results are displayed for the Light-Load condition in Figure 9(b).

4.4 Total Resistance of Vessel

We shall apply the results of Figure 9 and present a more complete analysis of the total resistance of the SES. This is shown in the two parts of Figure 10, for the two loading conditions, respectively.

Figure 10(a) compares the various theories detailed above with the experimental data for the total resistance of the model operated in the Full-Load condition. It is clear that applying the most sophisticated theory of seal resistance (the last curve in Figure 9(a), radically improves the correlation with the experimental data. Indeed, the discrepancy at the hump speed, between theory and experiment, has essentially been eliminated, if one can assume that the bow seal adopts a cubic profile.

In a similar manner, data for the Light-Load condition is presented in Figure 10(b). Again, one observes the most pleasing improvement in the predictions of the new theory in the hump region.

5 Optimization Studies

As a final exercise, we now compare the predictive ability of the new enhanced theory with data extracted from the optimization study performed on the model SES. The three parts of Figure 11 correspond to a separate study at each of three prototype speeds, of 18 knots, 20 knots, and 22 knots, respectively.

Figure 11(a) compares the resistance prediction from the various theories for the seal resistance with the model data for a speed of 18 knots. In this plot, the specific total resistance is plotted as a function of the cushion loading, which has been varied from 45% to 65%. In the physical experiment, this was achieved by carefully adjusting the cushion lift fans, in order to achieve the desired cushion lift. In this example, there is relatively little variation in resistance as the cushion pressure is varied.

On the other hand, Figure 11(b) — for a

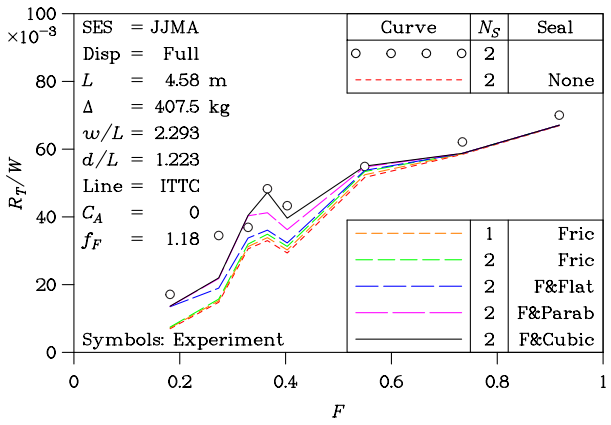

Figure 10: Total Resistance of Surface-Effect Ship (a) Full Displacement

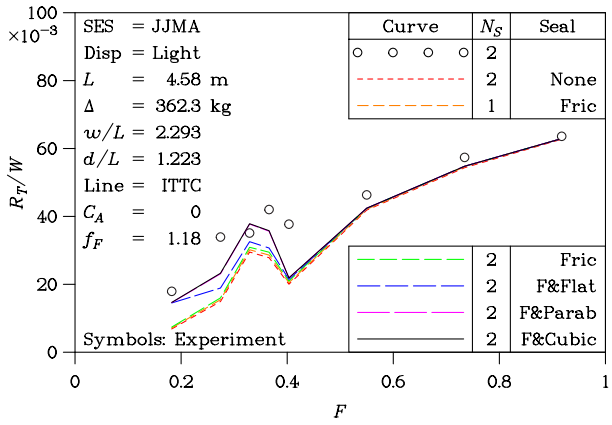

Figure 10: Total Resistance of Surface-Effect Ship (b) Light Displacement

speed of 20 knots — indicates a small drop in resistance as the cushion support increases from 45% to 60%. The theory is able to closely predict this behavior of the physical model SES. The slightly stronger influence of cushion loading, from 60% to 75% in Figure 11(c), for a speed of 22 knots, is also predicted well by the theory.

6 Concluding Remarks

6.1 Current Work

The research described in this paper has shown that:

1. The current hydrodynamic models for the stern seal and the bow seal give plausible and realistic corrections to the prediction of total resistance of an SES in the hump region.

2. The corrections for the seal resistance appear to lie between around 60% and 100% of the required values to bring the predictions into alignment with the experimental data for the model SES.

3. The frictional resistance on the seals is small compared to the total seal resistance at low speeds.

4. The hydrodynamic model in which the fingers of the bow seal are considered to deflect backwards as planing surfaces provides the major part of the seal resistance at these low speeds, in the form of pressure resistance. Nevertheless, one wonders if it were feasible to develop a simple model for the planing resistance — analogous to the formula for frictional resistance. This would be useful for spreadsheet computer programs.

5. The assumed profile of the deflected fingers is a significant factor.

6. This work confirms that of Steen and Adriaenssens (2005), in which it was noted that the resistance of the seals can constitute a significant component of the total resistance of a poorly trimmed SES.

6.2 Future Work

There is a number of avenues for extending this work in order to improve even further the accuracy of the resistance prediction:

1. It would be an interesting exercise to further study the effect of assuming different profiles of the deflected fingers of the bow seal. At this juncture, it is not clear how to select the appropriate profile without performing a first-principle analysis of the deflection of the fingers.

2. A further complication is that there remains the possibility of the fingers flagellating — this phenomenon has been observed on the rear seal. If this flagellation exists, it may increase

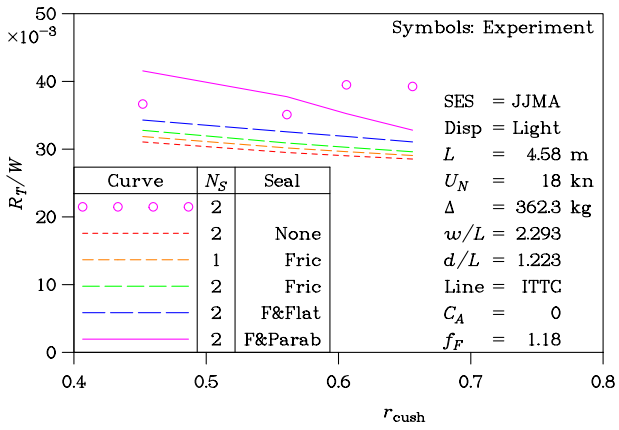

Figure 11: Influence of Cushion Lift on Resistance (a) Speed of 18 Knots

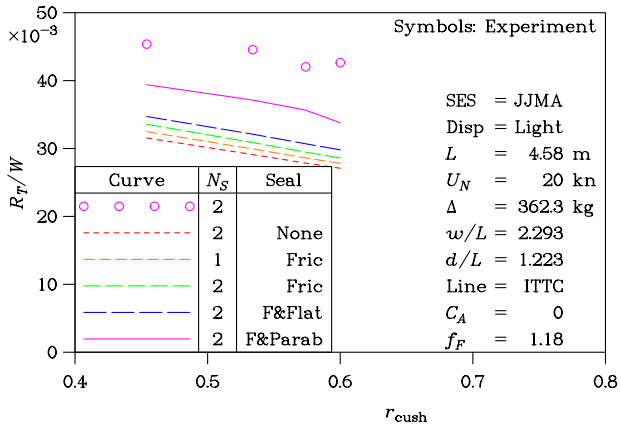

Figure 11: Influence of Cushion Lift on Resistance (b) Speed of 22 Knots

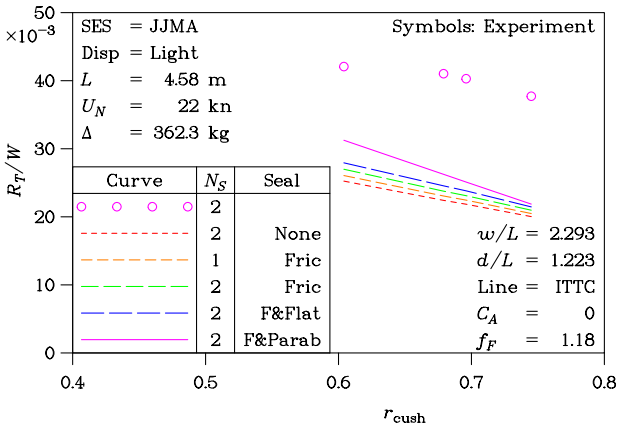

Figure 11: Influence of Cushion Lift on Resistance (c) Speed of 22 Knots

the bow-seal resistance beyond the value predicted through a simple steady-state analysis. If so, it would be most useful to be able to devise a "flagellation-onset predictor" parameter.

3. A more sophisticated analysis of the deflection of the fingers, taking into account their structural stiffness, could provide this information regarding their curvature. Perhaps a theory based on the work of Doctors (1978) would assist in this direction.

4. For a large SES, where the seals may be quite thick and robust, the weight of the seal may become important. This would apply particularly to the forward seal where the weight of the seal would exacerbate the demand for planing lift,

5. The convoluted nature of the fingers of the bow seal has been ignored in the current investigation. It would seem entirely reasonable to suggest that this feature would lower the lift-to-drag ratio of the bow seal. This would be another possible source of error which could be reduced in a future extension to this work. The two authors are not sure whether the two-dimensionality of the physics of the bow seal would increase or decrease as the number of fingers is increased. This problem could only be resolved with certainty through a more detailed analysis.

6. In the area of experimental work, it would be highly recommended to undertake measurements on a set of bow fingers in order to determine how realistic is the current theory proposed here. In this way, the correctness of the theory would be assessed directly, rather than indirectly through measurements on the total resistance of the SES.

   A photographic record of the deflected bow seal would constitute an excellent contribution to our understanding of the problem and would assist in the calibration of the theory. This is because it would allow us to check the estimate of the seal wetted length, which is a vital feature of the analysis. Actual measurements of the resistance suffered by the bow seal alone would provide further excellent data for corroborating the theory. This could be achieved by mounting the bow seal in a separate unit within the model and providing this unit with its own force-measurement system.

7 Acknowledgments

The support by JJMA Naval Architecture Division, Alion Science and Technology, is greatly appreciated. The experimental data for verifying the computer predictions constituted the essential element of this informative exercise.

The authors would like to acknowledge the assistance of the Australian Research Council (ARC) Discovery-Project Grant Scheme (via Grant Number DP0209656). This work was also partially supported by Office of Naval Research (ONR) contract N00014-05-1-0875. The in-kind support of this work from The University of New South Wales is also cheerfully acknowledged.

8 References

Broadbent, C. and Kennell, C.: "Monohull, Catamaran, Trimaran and SES High Speed Sealift Vessels", *Proc. Sixth International Conference on Fast Sea Transportation (FAST '01)*, Royal Institution of Naval Architects, Southampton, England, Vol. 1, pp 23–33 (September 2001)

Couser, P.R., Molland, A.F., Armstrong, N.A., and Utama, I.K.A.P.: "Calm Water Powering Predictions for High-Speed Catamarans", *Proc. Fourth International Conference on Fast Sea Transportation (FAST '97)*, Sydney, Australia, Vol. 2, pp 765–773 (July 1997)

de Vahl Davis, G.: *Numerical Methods in Engineering and Science*, Allen & Unwin (Publishers) Ltd, London, 286+xvi pp (1986)

Di Joseph, J.A., Heber, C.E., King, N., and Wilson, R.A.: "A Method of Scaling Model Drag Results for Surface Effect Ships", David W. Taylor Naval Ship Research and Development Center, Aviation and Surface Effects Department, Report ASED-342, 29+vi pp (September 1975)

Doctors, L.J.: "Representation of Planing Surfaces by Finite Pressure Elements", *Proc. Fifth Australasian Conference on Hydraulics and Fluid Mechanics*, Christchurch, New Zealand, Vol. 2, pp 480–488 (December 1974)

Doctors, L.J.: "Theory of Compliant Planing Surfaces and its Application to the Seals of a Surface-Effect Ship", David W. Taylor Naval Ship Research and Development Center, Aviation and Surface Effects Department, Report DTNSRDC-78/001, 162+viii pp (January 1978)

Doctors, L.J.: "On the Use of Pressure Distributions to Model the Hydrodynamics of Air-Cushion Vehicles and Surface-Effect Ships", *Naval Engineers J.*, Vol. 105, No. 2, pp 69–89 (March 1993)

Doctors, L.J.: "Optimal Pressure Distributions for River-Based Air-Cushion Vehicles", *Ship Technology Research: Schiffstechnik*, Vol. 44, No. 1, pp 32–36 (February 1997)

Doctors, L.J.: "Hydrodynamics of the Flow behind a Transom Stern", *Proc. Twenty-Ninth Israel Conference on Mechanical Engineering*, Paper 20-1, Technion, Haifa, Israel, 11 pp (May 2003)

Doctors, L.J. and Day, A.H.: "Wave-Free River-Based Air-Cushion Vehicles", *Proc. International Conference on Hydrodynamics of High-Speed Craft: Wake Wash and Motions Control*, Royal Institution of Naval Architects, London, England, pp 12.1–12.9 (November 2000)

Doctors, L.J., Renilson, M.R., Parker, G., and Hornsby, N.: "Waves and Wave Resistance of a High-Speed River Catamaran", *Proc. First International Conference on Fast Sea Transportation (FAST '91)*, Norwegian Institute of Technology, Trondheim, Norway, Vol. 1, pp 35–52 (June 1991)

Doctors, L.J. and Sharma, S.D.: "The Wave Resistance of an Air-Cushion Vehicle in Steady and Accelerated Motion", *J. Ship Research*, Vol. 16, No. 4, pp 248–260 (December 1972)

Doctors, L.J., Tregde, V., Jiang, C., and McKesson, C.B.: "Optimization of a Split-Cushion Surface-Effect Ship", *Proc. Eighth International Conference on Fast Sea Transportation (FAST '05)*, Saint Petersburg, Russia, 8 pp (June 2005)

Ford, A.G.: "Captured Air Bubble Over-Water Vehicle Concept", *Naval Engineers J.*, Vol. 76, No. 2, pp 223–230 (April 1964)

Ford, A.G., Bush, W.F., Wares, R.N., and Chorney, S.J.: "High Length-to-

Beam Ratio Surface Effect Ship", *Proc. AIAA/SNAME Advanced Marine Vehicles Conference*, San Diego, California, 15+i pp (April 1978)

Gabrielli, G. and von Kármán, T.: "What Price Speed?", *Mechanical Engineering*, Vol. 72, No. 10, pp 775–781 (October 1950)

Heber, C.E.: "Analysis of SES Model XR-1B Hump and Subhump Performance at Low Speeds. Phase II: In Head and Following Seas", Naval Ship Research and Development Center, Aviation and Surface Effects Department, Report 4474, 47+vi pp (September 1974)

Kennell, C.: "On the Nature of the Transport Factor Component TF_{ship}", *Marine Technology*, Vol. 38, No. 2, pp 106–111 (April 2001)

Layton, D.M.: "The Effects of Bow Seal Shape on the Performance of a Captured Air Bubble Surface Effect Ship", *Proc. AIAA/SNAME Advanced Marine Vehicles Conference*, Arlington, Virginia, 5+i pp (September 1976)

Lewis, E.V. (Ed.): *Principles of Naval Architecture: Volume II. Resistance, Propulsion and Vibration*, Society of Naval Architects and Marine Engineers, Jersey City, New Jersey, 327+vi pp (1988)

Malakhoff, A. and Davis, S.: "Dynamics of SES Bow Seal Fingers", *Proc. American Institute of Aeronautics and Astronautics Sixth Marine Systems Conference*, Seattle, Washington, 13+i pp (September 1981)

Maruo, H.: "Two Dimensional Theory of the Hydroplane", *Proc. First Japan National Congress for Applied Mechanics*, pp 409–415 (1951)

Michell, J.H.: "The Wave Resistance of a Ship", *Philosophical Magazine*, London, Series 5, Vol. 45, pp 106–123 (1898)

Newman, J.N. and Poole, F.A.P.: "The Wave Resistance of a Moving Pressure Distribution in a Canal", *Schiffstechnik*, Vol. 9, No. 45, pp 21–26 (1962)

Sahoo, P.K. and Doctors, L.J.: "A Study on Wave Resistance of High-Speed Displacement Hull Forms in Restricted Depth", *Proc. Seventh International Conference on Fast Sea Transportation (FAST '03)*, Ischia, Italy, Vol. 1, pp A3.25–A3.32 (October 2003)

Squire, H.B.: "The Motion of a Simple Wedge along the Water Surface", *Proc. Royal Society of London*, Series A, Vol. 243, No. 1232, pp 48–64 (1957)

Sretensky, L.N.: "On the Motion of a Glider on Deep Water", *Bulletin of the USSR Academy of Sciences*, Department of Mathematical and Natural Sciences, pp 817–835 (1933)

Steen, S.: "Calm Water Resistance Testing of LCS SES: Resistance Test of C-Version", Marintek Norwegian Marine Technology Research Institute, Trondheim, Norway, Report 530020.00.01, 43 pp (April 2004)

Steen, S. and Adriaenssens, C.: "Experimental Verification of the Resistance of a Split-Cushion Surface-Effect Ship", *Proc. Eighth International Conference on Fast Sea Transportation (FAST '05)*, Saint Petersburg, Russia, 8 pp (June 2005)

Templeman, M. and Kennell, C.: "The Effect of Ship Size on Transport Factor Properties", *Proc. First International Conference on High-Performance Marine Vehicles (HIPER '99)*, Zevenwacht, South Africa, pp 210–219 (March 1999)

Van Dyck, R.L. and Fridsma, G.: "The Contribution of Seals and Sidewalls to the Force and Moment Characteristics of an SES", Stevens Institute of Technology, Davidson Laboratory, Report SIT-DL-79-1861, 127+iii pp (April 1979)

Wilson, R.A., Wells, S.M., and Heber, C.E.: "Powering Predictions for Surface Effect Ships Based on Model Results", *J. Hydronautics*, Vol. 13, No. 4, pp 113–119 (October 1979)